Regulation of Transcription through Light-Activation and Light-Deactivation of Triplex-Forming Oligonucleotides in Mammalian Cells

ARTICLE *in* ACS CHEMICAL BIOLOGY · APRIL 2012

Impact Factor: 5.33 · DOI: 10.1021/cb300161r · Source: PubMed

5 AUTHORS, INCLUDING:

Jeane M Govan
University of Texas MD Anderson Cancer Center
11 PUBLICATIONS **141** CITATIONS
SEE PROFILE

Rajendra Uprety
Memorial Sloan-Kettering Cancer Center
12 PUBLICATIONS **191** CITATIONS
SEE PROFILE

Alexander Deiters
University of Pittsburgh
135 PUBLICATIONS **4,970** CITATIONS
SEE PROFILE

ACS chemical biology

Articles

pubs.acs.org/acschemicalbiology

Regulation of Transcription through Light-Activation and Light-Deactivation of Triplex-Forming Oligonucleotides in Mammalian Cells

Jeane M. Govan,[†] Rajendra Uprety,[†] James Hemphill,[†] Mark O. Lively,[‡] and Alexander Deiters*[,†]

[†]Department of Chemistry, North Carolina State University, Raleigh, North Carolina 27695, United States

[‡]Center for Structural Biology, Wake Forest University School of Medicine, Winston-Salem, North Carolina 27157, United States

Supporting Information

ABSTRACT: Triplex-forming oligonucleotides (TFOs) are efficient tools to regulate gene expression through the inhibition of transcription. Here, nucleobase-caging technology was applied to the temporal regulation of transcription through light-activated TFOs. Through site-specific incorporation of caged thymidine nucleotides, the TFO:DNA triplex formation is blocked, rendering the TFO inactive. However, after a brief UV irradiation, the caging groups are removed, activating the TFO and leading to the inhibition of transcription. Furthermore, the synthesis and site-specific incorporation of caged deoxycytidine nucleotides within TFO inhibitor sequences was developed, allowing for the light-deactivation of TFO function and thus photochemical activation of gene expression. After UV-induced removal of the caging groups, the TFO forms a DNA dumbbell structure, rendering it inactive, releasing it from the DNA, and activating transcription. These are the first examples of light-regulated TFOs and their application in the photochemical activation and deactivation of gene expression. In addition, hairpin loop structures were found to significantly increase the efficacy of phosphodiester DNA-based TFOs in tissue culture.

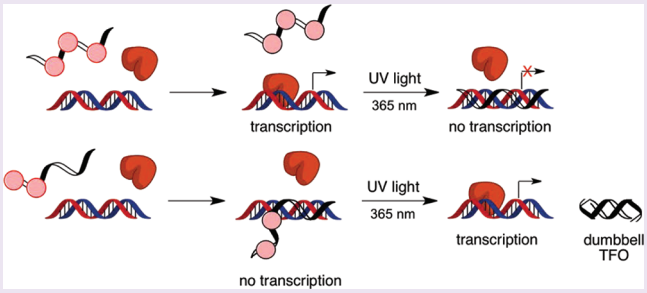

Triplex-forming oligonucleotides (TFOs) bind double-stranded DNA in a sequence-specific manner for a variety of different functions and applications, including the inhibition of protein–DNA binding,[1] gene expression,[2] and DNA replication.[3] TFOs have also been applied to induce site-specific DNA damage,[4] to enhance DNA recombination,[5] and to perform DNA mutagenesis.[6,7] Recently, TFOs have even been used as electrochemical sensors for double-stranded DNA.[8] Currently, TFOs and decoy oligonucleotides are one of the few gene-regulating tools used to inhibit transcription, in contrast to traditional antisense agents that regulate translation of a given gene. TFOs block transcription factors from binding to their genomic recognition site by forming a DNA triplex structure within a promoter sequence (Figure 1),[9] whereas decoy oligonucleotides directly sequester the target transcription factors.[10] One advantage of TFOs over RNA-targeting antisense agents in the regulation of gene expression is the lower copy number of genomic DNA compared to the higher copy number of mRNA.[6]

TFOs are single-stranded oligonucleotides that can recognize polypurine- or polypyrimidine-rich regions of double-stranded DNA by binding in the major groove of DNA through Hoogsteen hydrogen bonds.[1,11] For example, adenine can hybridize to an adenine:thymine base pair forming an T:A:T triplex (Figure 1B), while guanine can bind through reverse Hoogsteen hydrogen bonds to a guanine:cystosine base pair forming a G:G:C triplex structure (Figure 1C).[2,6,7,12]

One current limitation of TFOs is that their activity cannot be controlled with spatial or temporal resolution, thus preventing their application in the precise dissection of biological processes. A solution to this problem can be found in "caging" technologies that have been developed to photochemically regulate biological function with high spatiotemporal resolution.[13−20] By placing a photolabile protecting group ("caging" group) onto the base of a nucleotide, its ability to undergo hybridization is disrupted, rendering the oligonucleotide functionally inactive. After brief UV irradiation, the caging groups are cleaved, and oligonucleotide activity is restored.[21−25] Here, we demonstrate that this methodology can be extended to the photochemical regulation of Hoogsteen base-pairing and thus the activation and deactivation of TFO function and gene transcription in live cells.

Cyclin D1 was selected as a model system for the design of light-controlled TFOs because of its critical regulatory role in the cell cycle.[26−28] Cyclin D1 is essential in the transition from G_1 to S phase in the cell cycle, and the misregulation of this process has been associated with a number of neoplastic diseases.[29,30] Overexpression of cyclin D1 causes multiple

Received: October 18, 2011
Accepted: April 27, 2012

   dx.doi.org/10.1021/cb300161r | *ACS Chem. Biol.* XXXX, XXX, XXX–XXX

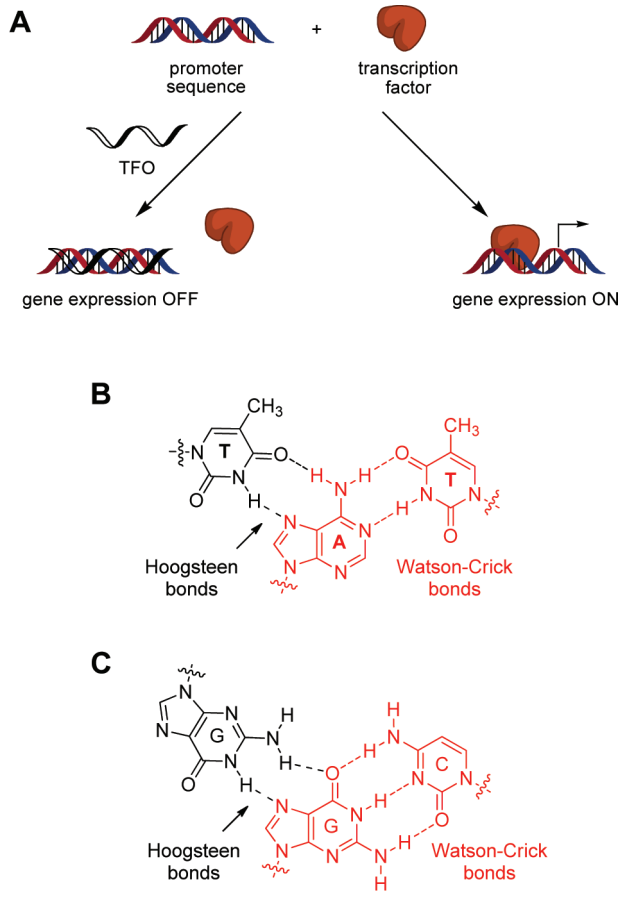

Figure 1. (A) General mechanism of gene silencing by triplex-forming oligonucleotides (TFOs) targeting promoter sequences. The presence of a DNA triplex in the promoter region prevents transcription factor binding and silences gene expression. (B) Hydrogen bond formation between the A:T pair in duplex DNA (red) and a T in the TFO. (C) Reverse hydrogen bond formation between the G:C pair in duplex DNA (red) and a G in the TFO.

downstream effects, including anchorage-independent growth, vascular endothelial growth factor production, tumorigenicity in mice, and resistance to chemotherapeutic agents.[30] Inhibition of cyclin D1 translation[31] and transcription[32] has been achieved with oligonucleotides and, in combination with chemotherapeutic agents (*e.g.*, 5-fluorourcil, methotrexate, and cisplatin), enhances the overall effect of cancer treatment.[31,33]

RESULTS AND DISCUSSION

In order to demonstrate photochemical control of TFO function, noncaged deoxyoligonucleotides and caged deoxyoligonucleotides containing 6-nitropiperonyloxymethyl (NPOM)-caged thymidine residues were synthesized (Table 1), based on successful applications of caged thymidines in the light-regulation of DNA function.[24,25,34−36] These TFO sequences specifically target the cyclin D1 promoter, as previously reported.[32] Although they are not canonical homopurines or homopyrimidines, there is evidence that mixed-purine/pyrimidine G-rich TFOs can exhibit sufficient binding to double-stranded DNA targets.[37] Despite the G-rich nature of the cyclin D1 TFO, G-rich TFOs are highly active antigene agents that bind to double-stranded genomic DNA targets and efficiently inhibit transcription.[38−40] First, noncaged TFOs were synthesized in order to validate efficient gene silencing. A TFO with a nonmodified phosphodiester backbone (TFO-1) and, in order to stabilize the oligonucleotide for intracellular applications, a TFO containing phosphorothioate modifications (PS-TFO-1) were synthesized.[41,42] In addition, hairpin loop structures on the 5′ and 3′ termini of antisense agents have recently been shown to stabilize oligonucleotides in tissue culture while maintaining their antisense properties,[34,43] a methodology that has previously not been applied to TFOs. Thus, a hairpin-protected TFO composed of regular DNA containing phosphodiester linkages was also generated (HP-TFO-1). The inactive TFOs TFO-0, PS-TFO-0, and HP-TFO-0 were designed as negative control oligonucleotides and were synthesized.

Table 1. Structure of the Caged Thymidine Residue and Sequences of Synthesized Triplex-Forming Oligonucleotides (TFOs)[a]

DNA	Sequence
Target Duplex	5′ CCCCTGCGCCCGCCCCCGCCCCCCTCCCGC 3′ GGGGACGCGGGCGGGGGCGGGGGGAGGGCG
TFO-0	5′ CACCCACCCCCACCCCCC
TFO-1	5′ GTGGGTGGGGGTGGGGGG
PS-TFO-0	5′ C*A*C*C*C*A*C*C*C*C*C*A*C*C*C*C*C*C
PS-TFO-1	5′ G*T*G*G*G*T*G*G*G*G*G*T*G*G*G*G*G*G
HP-TFO-0	A GCGCGCG 5′ GCGCGCG A A CGCGCGCTACCACCCACCCCCACCCCCCTATCGCGCGC A A A
HP-TFO-1	A GCGCGCG 5′ GCGCGCG A A CGCGCGCTACGTGGGTGGGGGTGGGGGGTATCGCGCGC A A A
CHP-TFO-1	A GCGCGCG 5′ GCGCGCG A A CGCGCGCTACG**T**GGG**T**GGGGG**T**GGGGGG**T**ATCGCGCGC A A A

[a]Asterisk (*) denotes a phosphorothioate bond, and **T** denotes a caged thymidine (see insert).

dx.doi.org/10.1021/cb300161r | *ACS Chem. Biol.* XXXX, XXX, XXX−XXX

Gel shift assays were performed in order to examine if the backbone modifications or the introduction of the hairpin loop structures has an effect on the formation of oligonucleotide triplexes. Gratifyingly, the phosphodiester TFO-1, phosphorothioate PS-TFO-1, and the hairpin-protected HP-TFO-1 efficiently bind to the cyclin D1 duplex DNA target to form triplex structures, inducing a corresponding gel shift (Figure 2,

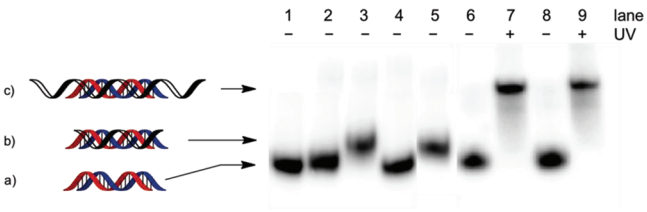

Figure 2. Investigation of triplex formation *via* gel shift assays. The radiolabeled cyclin D1 target sense strand was annealed to its complement and was incubated with a 5-fold excess of TFO at 37 °C for 4 h. Lane 1: Cyclin D1 target duplex. Lane 2: TFO-0. Lane 3: TFO-1. Lane 4: PS-TFO-0. Lane 5: PS-TFO-1. Lane 6: HP-TFO-0. Lane 7: HP-TFO-1. Lane 8: CHP-TFO-1 −UV. Lane 9: CHP-TFO-1 + UV. (a) Unbound DNA duplex. (b) DNA duplex bound to a TFO. (c) DNA duplex bound to a hairpin-protected TFO.

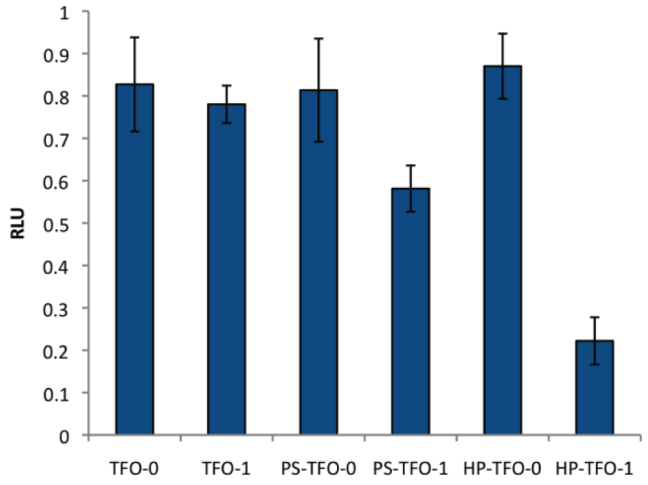

Figure 3. Intracellular inhibition of cyclin D1 promoter-driven transcription using modified TFOs. HEK 293T cells were co-transfected with pCyclin-D1 Δ-944, pRL-TK, and TFOs. Relative luciferase units (RLU) represent the firefly luciferase signal under control of the cyclin D1 promoter normalized to the *Renilla* luciferase signal as a control. Error bars represent standard deviations from three independent experiments.

lanes 3, 5, and 7). As expected, the negative control TFOs TFO-0, PS-TFO-0, and HP-TFO-0 did not form triplex structures, as evident by the lack of a shifted radiolabeled target DNA. Since no difference in triplex-forming ability was observed between the phosphodiester and phosphorothioate-modified oligonucleotides, both species were subsequently tested in mammalian tissue culture.

Next, the effect of triplex formation on cyclin D1-driven expression of a luciferase reporter gene in live cells was investigated. TFOs were transfected into human embryonic kidney (HEK) 293T cells together with a dual reporter system encoding firefly luciferase and *Renilla* luciferase. The cyclin D1 promoter was present upstream of the firefly luciferase gene (pCyclin D1 Δ-944),[44] enabling the measurement of promoter activity by quantifying firefly luciferase expression. The *Renilla* luciferase plasmid (pRL-TK) was used as a control to account for differences in cell viability and transfection efficiency. As expected on the basis of the gel shift assays shown in Figure 2, the negative controls (TFO-0 and PS-TFO-0) showed no inhibition of firefly luciferase expression (Figure 3). Also, TFO-1, which consists of DNA with a simple phosphodiester linkage, showed no inhibition of firefly gene expression. This is most likely the result of fast intracellular degradation of the TFO, since unmodified DNA is quickly degraded by exonucleases.[45] Surprisingly, the substantially more stable phosphorothioate PS-TFO-1 led to only a marginal inhibition (25−40%) of firefly luciferase expression, despite optimization of transfection conditions (see Supporting Information, Figures 1 and 2). This low level of transcriptional inhibition could potentially be the result of TFO sequestering through nonspecific binding of the phosphorothioate DNA to proteins[7] or the result of PS-TFO:DNA triplexes having a dissociation constant 10-fold higher than that of phosphodiester TFO:DNA triplexes.[46] Importantly, the hairpin-protected TFO (HP-TFO-1) induced a >70% inhibition of luciferase expression, while the corresponding negative control HP-TFO-0 showed no gene knockdown. This demonstrated, for the first time, that hairpin-stabilized deoxyoligonucleotides containing regular phosphodiester bonds could be effectively applied as triplex-forming gene regulatory agents in mammalian cell culture.

Since HP-TFO-1 demonstrated the greatest inhibition of gene transcription, we synthesized a corresponding caged analogue (CHP-TFO-1). On the basis of previous studies investigating the effect of multiple caged thymidines on the inhibition of Watson−Crick base-pairing in DNA:DNA and DNA:RNA duplexes,[24,25] caged thymidine nucleotides were incorporated every 3−6 nucleotides throughout the TFO binding site in HP-TFO-1, generating CHP-TFO-1 bearing four NPOM caging groups (Table 1). To determine if the caged hairpin TFO forms a triplex structure, a gel shift assay was performed. Gratifyingly, the installation of 4 caging groups on selected thymidine residues completely prevented CHP-TFO-1 from undergoing DNA triplex formation (Figure 2, lane 8), as the gel shows only a band for the unbound cyclin D1 target duplex. CHP-TFO-1 is as inactive as the corresponding negative control TFO HP-TFO-0 (lane 6). However, upon UV irradiation the caging groups are removed and the hairpin TFO binds to the cyclin D1 target site forming a triplex structure and induces a significant gel shift (lane 9), identical to the shift observed for the positive control TFO shown in lane 7 (HP-TFO-1).

These results set the stage for the investigation of the light-activation of the caged hairpin TFO in cell culture. We hypothesized that the caged CHP-TFO-1 would be inactive when transfected into mammalian cells, leading to gene expression. A brief UV irradiation, however, will remove the caging groups, activate the TFO, and lead to the suppression of gene expression (Figure 4A). To this end, HEK 293T cells were co-transfected with plasmids encoding firefly luciferase (pCyclin D1 Δ-944), *Renilla* luciferase (pRL-TK), and with the TFO antisense agents. As expected, the negative control hairpin HP-TFO-0 had no effect on firefly luciferase activity regardless of UV irradiation (Figure 4B). HP-TFO-1 reduced luciferase expression by approximately 80%, in agreement with the previous assay (Figure 3). The caged hairpin TFO (CHP-TFO-1) was inactive, showing full luciferase expression

dx.doi.org/10.1021/cb300161r | *ACS Chem. Biol.* XXXX, XXX, XXX−XXX

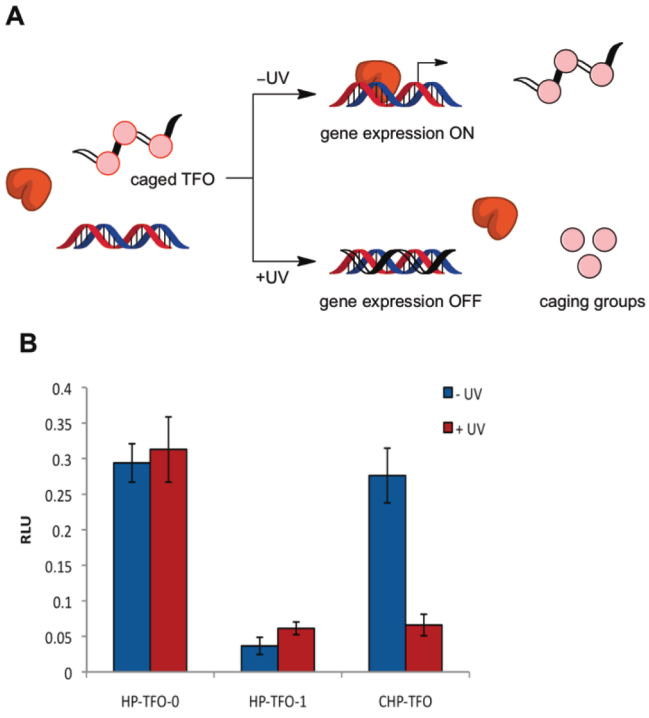

Figure 4. Photochemical activation of caged TFOs in mammalian cells. (A) Schematic of light-activated gene silencing using caged TFOs. The sequence of the TFO that binds to the targeted double-stranded DNA is blocked through light-removable protecting groups (caging groups). UV irradiation removes the caging groups, restores TFO activity, and inhibits gene expression. (B) Dual-Luciferase reporter assay in the presence and absence of UV irradiation (365 nm, 2 min). Relative luciferase units (RLU) represent the firefly luciferase signal under control of the cyclin D1 promoter normalized to the *Renilla* luciferase signal as a control. Error bars represent standard deviations from three independent experiments.

(comparable to the negative control HP-TFO-0) and demonstrating that intracellular triplex formation and thus gene silencing could be completely inhibited through the installation of nucleobase caging groups at defined thymidine residues. After brief UV irradiation (365 nm) of the transfected HEK 293T cells, the caging groups were removed, triplex-forming ability was restored, and a 78% inhibition of gene expression was observed, comparable to that of the noncaged HP-TFO-1. The optimal irradiation condition was found to be 2 min, and no increased inhibition was observed with prolonged exposure to UV light (see Supporting Information, Figure S3). The resulting level of reporter gene activity before and after UV irradiation demonstrates a highly efficient light-switching of an inactive, caged TFO (CHP-TFO-1) to a fully active, transcription-inhibiting TFO (HP-TFO-1).

In addition to the photochemical activation of TFOs and thus photochemical inhibition of transcription, we hypothesized that by designing a caged TFO dumbbell structure we can achieve *photochemical inhibition* of TFO activity and therefore light-activation of transcription. In the caged form, the TFO dumbbell will bind DNA, forming a triplex structure and thereby inhibiting gene expression. After irradiation, the caging groups are cleaved and the TFO will now deactivate itself by forming a DNA dumbbell structure that cannot bind to the promoter region anymore, leading to an activation of gene expression (Figure 5).

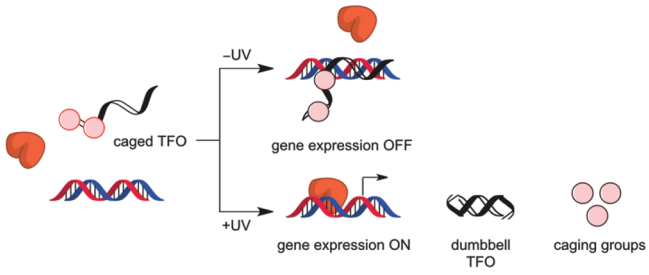

Figure 5. Schematic of the light-activation of gene expression (gene transcription) using caged dumbbell TFOs. The TFO is active before UV irradiation and becomes inactive through decaging and subsequent blocking of the double-stranded DNA targeting site by dumbbell formation.

Due to the prevalence of guanines in the TFO targeting region, the caged thymidine phosphoramidite could not be applied, and a caged deoxycytidine phosphoramidite (Figure 6) needed to be developed in order to create a light-deactivatable TFO. Previously, 1-(2-nitrophenyl) ethyl caged deoxycytidine

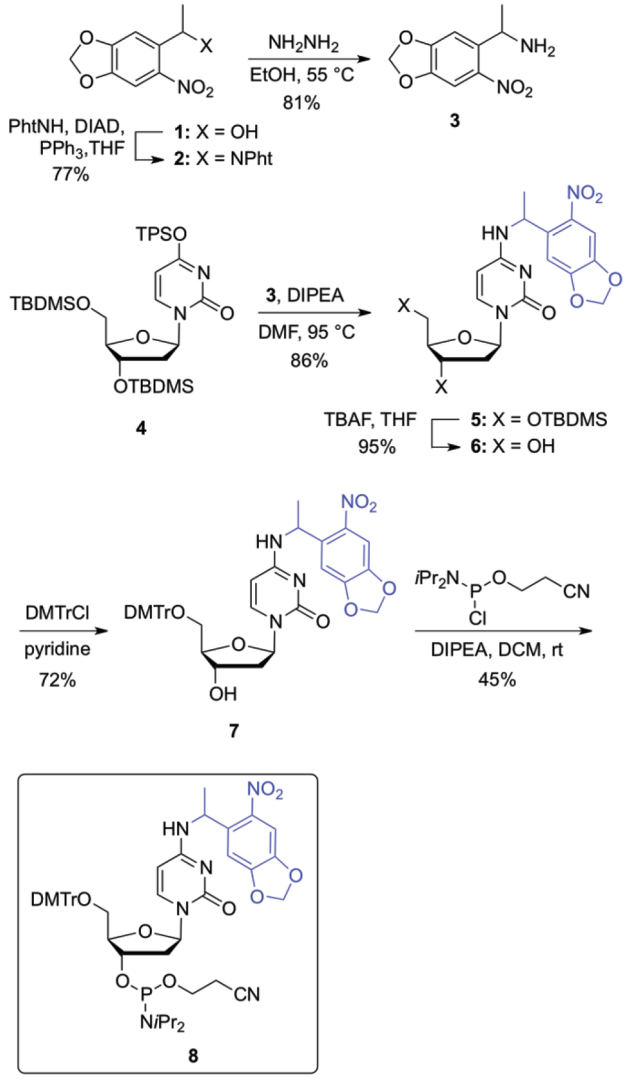

Figure 6. Synthesis of the nitropiperonyl ethyl (NPE)-caged deoxycytidine phosphoramidite **8**. The light-removable caging group is shown in blue. PhtNH = phtalimide, TPS = triisopropylbenzene-sulfonyl, TBDMS = *tert*-butyldimethylsilyl, DMTr = dimethoxytrityl.

dx.doi.org/10.1021/cb300161r | *ACS Chem. Biol.* XXXX, XXX, XXX–XXX

Table 2. Structure of the Caged Cytidine Residue and Sequences of Synthesized Triplex-Forming Oligonucleotides[a]

DNA	Sequence
DB-TFO-1	5′ 3′ A A GCGCGCGATGCACCCACCCCCACCCCCCATAGCGCGCG A A CGCGCGCTACGTGGGTGGGGGTGGGGGGTATCGCGCGC A A
CDB-TFO-1	3′-ATGCACCCACCCCCACCCCCATA GCGCGCG A A GCGCGCG-5′ A A CGCGCGCTACGTGGGTGGGGGTGGGGGGTATCGCGCGC A
CDB-TFO-2	3′-ATGCACCCACCCCCACCCCCATAGCGCGCG A A GCGCGCG-5′ A A CGCGCGCTACGTGGGTGGGGGTGGGGGGTATCGCGCGC A

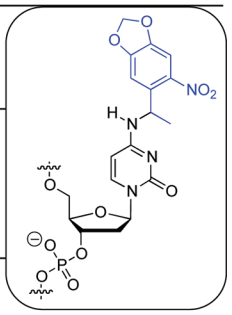

[a]C denotes a caged cytidine nucleotide (see insert).

has been synthesized and used in the activation of aptamers using light.[47] However, it has been shown that the efficiency of photolysis of the 2-nitrobenzyl caging group depends upon the nature of its aromatic substituents.[48] Electron-rich substituents on the benzene ring and a methyl substituent in the benzylic position enhance the photolytic properties of such caging groups, enabling the use of long-wavelength UV light of 365 nm, and thus are advantageous for applications in biological systems.[49,50] In order to take advantage of the electron-donating nature of the methylenedioxy moiety and the α-methyl group, a nitropiperonyl ethyl (NPE)-caged deoxycytidine phosphoramidite was designed for the synthesis of caged DNA oligonucleotides containing light-activatable deoxycytidine residues. The synthesis of the caged phosphoramidite **8** commenced with the coupling of phthalimide with the known alcohol[51] **1** in the presence of diisopropyl azodicarboxylate and triphenylphosphine in THF, affording the corresponding nitrodione **2** in 77% yield.[52] The dione **2** was reacted with hydrazine in refluxing ethanol for 2 h, delivering the amine **3** in 81% yield. The amine **3** was subsequently coupled with TBDMS-protected triisopropylbenzenesulfonyl activated deoxyuridine **4** (synthesized in 2 steps from 2′ deoxyuridine)[53] in the presence of diisopropyl ethyl amine (DIPEA) in DMF at reflux conditions for 12 h to obtain the NPE-caged deoxycytidine nucleoside **5** in 86% yield. The TBDMS groups on **5** were removed through treatment with TBAF in tetrahydrofuran at low temperature to give the corresponding alcohol **6** (95% yield). Selective tritylation of the 5′ hydroxyl group of **6** with dimethoxytritylchloride in pyridine was carried out at RT and delivered the compound **7** in 72% yield. Finally, activation of the 3′ hydroxyl group of **7** was achieved by reacting it with 2-cyanoethyl *N*,*N*-diisopropylchlorophosphoramidite in the presence of DIPEA in dichloromethane providing the desired caged deoxycytidine phosphoramidite **8** as a white solid in 45% yield.

In order to test the photochemical activation of gene expression with light-deactivatable TFOs, the corresponding noncaged DNA oligonucleotides and caged DNA oligonucleotides containing NPE-protected cytidine residues were synthesized (Table 2). The caged cytidine nucleotides were site-specifically incorporated every 3−4 bases along the self-complementary inhibitor sequence of the TFO molecule. This design renders the TFO binding site open to hybridization to its double-stranded DNA target in the caged form; however, UV irradiation will remove the caging groups, inducing formation of a dumbbell structure that blocks the binding site and deactivates TFO function. In turn, this leads to the light-activation of transcription. On the basis of our results with the hairpin TFO (HP-TFO-1) described above, the hairpin loop structures were incorporated into the TFO to provide cellular stability to the DNA.

The light-deactivation of TFOs was first investigated using a gel shift assay (Figure 7). The radiolabeled double-stranded

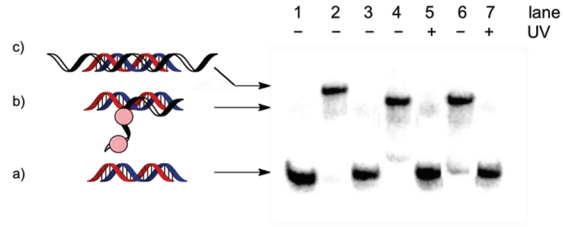

Figure 7. Investigation of triplex formation *via* gel shift assays. The ^{32}P-radiolabeled cyclin D1 target duplex DNA was incubated with the different TFOs at 37 °C for 2 h. Lane 1: Cyclin D1 target duplex. Lane 2: HP-TFO-1. Lane 3: DB-TFO-1. Lane 4: CDB-TFO-1 −UV. Lane 5: CDB-TFO-1 +UV. Lane 6: CDB-TFO-2 −UV, Lane 7: CDB-TFO-2 +UV. (a) Unbound radiolabeled DNA duplex. (b) DNA duplex bound to an active, caged dumbbell TFO (CDB-TFO). (c) DNA duplex bound to a hairpin TFO.

cyclin D1 target sequence was incubated with the noncaged or caged TFOs. The caged dumbbell TFOs were either kept in the dark or were irradiated for 5 min (365 nm). As a positive control, the HP-TFO-1 was used and displayed a significant gel shift indicating the formation of a triplex structure (Figure 7, lane 2) when compared to just the target DNA duplex (lane 1). In the presence of the dumbbell TFO, DB-TFO-1, no gel shift was observed (lane 3), indicating that the double-stranded stem of the TFO does not bind to the target and does not form a triplex structure. The caged TFOs, CDB-TFO-1 and CDB-TFO-2, containing 4 or 5 caged cytidine nucleotides, however, do in fact bind the targeted DNA duplex and form triplex structures (lanes 4 and 6), since dumbbell formation is inhibited by the presence of the caging groups. However, after light irradiation, the caging groups are removed leading to formation of the dumbbell and thus inhibition of TFO binding activity (lanes 5 and 7).

dx.doi.org/10.1021/cb300161r | *ACS Chem. Biol.* XXXX, XXX, XXX−XXX

The gel shift results indicate the potential to photochemically deactivate triplex-formation and thus photochemically activate transcription. Thus, the noncaged and caged dumbbell TFOs were tested in cell culture. HEK 293T cells were co-transfected with plasmids encoding firefly luciferase (pCyclin D1 Δ-944), *Renilla* luciferase (pRL-TK), and with the TFOs. As a positive control for UV exposure, the CHP-TFO-1 was used since we have already established that it has an excellent light-switching behavior from an inactive to an active TFO (see Figure 4). As before, the CHP-TFO-1 shows no inhibition of gene expression until irradiation induces decaging and virtually complete inhibition of luciferase expression (Figure 8). The dumbbell

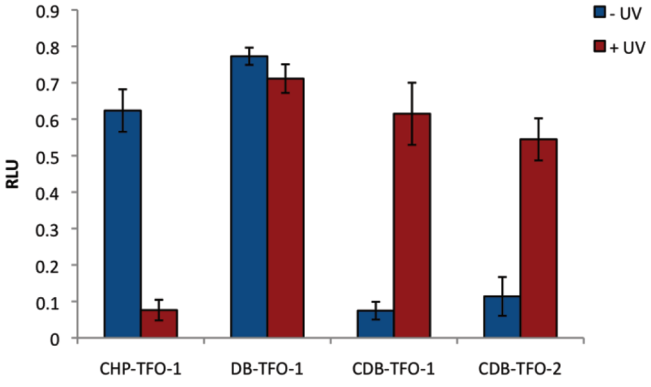

Figure 8. Photochemical activation of gene transcription in mammalian cells. Relative luciferase units (RLU) represent the firefly luciferase signal normalized to a *Renilla* luciferase signal as a transfection and cell viability control. Error bars represent standard deviations from three independent experiments.

TFO DB-TFO-1 does not inhibit gene expression, as expected, based on the gel shift results (see Figure 7). Gratifyingly, the CDB-TFO-1 is an active TFO, inhibiting luciferase transcription until irradiated with UV light of 365 nm (5 min), which removes the caging groups and deactivates the TFO through dumbbell formation, leading to a substantial increase in luciferase activity. Similarly, the CDB-TFO-2 (carrying 5 caging groups) inhibits gene expression before irradiation followed by restoration of gene expression after a brief UV exposure. These results demonstrate that the caged dumbbell TFOs are complementary tools to the caged TFOs. Together they enable the promoter-specific light-activation and light-deactivation of transcription with excellent efficiency, allowing caged TFOs to be used as photochemical on/off switches for gene function.

On the basis of the successful light-activation and light-deactivation of gene activity in a classical luciferase reporter system, the caged TFOs were subsequently tested for their photochemical regulation of the endogenous cyclin D1 gene. Due to the tightly packed nature of chromatin DNA compared to plasmid DNA, the light regulation of an endogenous gene using caged TFOs needed to be validated. Toward this goal, the human breast cancer cell line (MDA-MB-231) was transfected with the previously synthesized caged TFOs, and cells were either irradiated (365 nm) or kept in the dark. After 48 h, cellular RNA was isolated and subjected to quantitative real-time PCR (qRT PCR) analysis. Serving as a negative control, HP-TFO-0 displayed no inhibition of cyclin D1 expression, while HP-TFO-1 suppressed cyclin D1 expression by 80% (Figure 9). Thus, the inhibition of expression of an endogenous gene is in good agreement with inhibition of reporter gene expression. The caged hairpin-stabilized TFO CHP-TFO-1 was

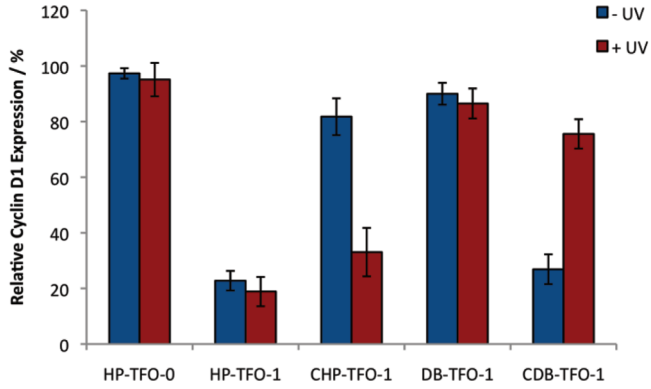

Figure 9. Photochemical activation and deactivation of cyclin D1 expression in mammalian cells. MBA-MD-231 cells were transfected with TFOs, and cells were incubated for 48 h at 37 °C. RNA was isolated, and qRT PCR quantification was performed. Cyclin D1 expression was normalized to the expression of the GAPDH housekeeping gene, and expression levels in untreated cells were set to 100%. Error bars represent standard deviations from three independent experiments.

inactive; however, activity was restored through UV irradiation (5 min, 365 nm) leading to a light-induced knock-down of an endogenous gene. In order to demonstrate photochemical activation of cyclin D1 gene expression, the caged active TFO, CDB-TFO-1, was transfected into MDA-MB-231 cells. The 4 caging groups present in the predumbbell TFO CDB-TFO-1 rendered this silencing agent active with 74% suppression of cyclin D1 expression. Upon UV irradiation, the dumbbell is formed, inactivating the TFO and activating gene expression. The application of the two caged oligonucleotides, CHP-TFO-1 and CDB-TFO-1, demonstrates for the first time the light-activation and light-deactivation of transcription of an endogenous gene. Thus, the developed nucleobase-caging technology is highly versatile and can be applied to any TFO target site, as caged phosphoramidites of all four nucleotides are available.[36,53,54] This methodology will enable transcriptional studies of gene expression with high spatial and temporal resolution using caged TFOs.

Summary. Caged triplex-forming oligonucleotides (TFOs) were synthesized and successfully applied in the photochemical regulation – activation and deactivation – of transcription in mammalian cells. In the course of these studies, several important discoveries and methodology advancements were made. Specifically, the first physiologically active TFOs composed of standard DNA and stabilized with intramolecular hairpins at the 5′ and 3′ termini were synthesized. These reagents enabled stronger inhibition of gene expression than standard phosphorothioate-stabilized TFOs. Through the direct incorporation of caging groups on nucleobases within the TFO molecules, light-induced inhibition of a specific promoter (cyclin D1) and thus inhibition of gene transcription was achieved. Gel shift studies verified that the installed caging groups disrupt reverse Hoogsteen hydrogen bonding of the TFO to the target DNA duplex and that binding can be restored through decaging and activation of the TFO *via* a brief UV irradiation. In addition, a caged TFO design was developed that enables the light-activation of gene expression. This was achieved through the synthesis of a new caged deoxycytidine phosphoramidite and its incorporation into dumbbell-forming TFOs. Here, the TFO molecule is active and inhibits transcription until UV irradiation renders it inactive through

dx.doi.org/10.1021/cb300161r | *ACS Chem. Biol.* XXXX, XXX, XXX–XXX

nucleobase decaging and DNA dumbbell formation, leading to light-activation of transcription. These methodologies were validated in human cells by photochemically controlling the transcription of a transiently transfected reporter gene (luciferase) and an endogenous gene (cyclin D1).

TFOs are versatile inhibitors of transcription and have been applied to the knock-down of a wide range of genes,[12,55] despite several factors that may limit their applicability, including electrostatic repulsion between the three negatively charged DNA strands, limited sequence variation, and the potential formation of secondary DNA structures.[55,56] However, several nucleotide modifications have been developed for enhanced triplex stabilization, inhibition of secondary structures, and improved binding affinity[57,58] and could be combined with this caging technology to further improve its applicability in tissue culture and in model organisms.

The discoveries reported here, intracellular function of DNA-based TFOs through stabilization by terminal hairpins and their photochemical activation and deactivation using caged nucleobases, have implications in the precise regulation of gene promoter activity in tissue culture and multicellular organisms.[59,60] Applications of caged TFOs range from basic biological studies of gene expression to new gene therapeutic approaches in high spatial and temporal resolution.

METHODS

DNA Synthesis Protocol. DNA synthesis was performed using an Applied Biosystems Model 394 automated DNA/RNA synthesizer and standard β-cyanoethyl phosphoramidite chemistry. The caged hairpin triplex-forming oligonucleotide was synthesized on a 40 nmol scale, with a low volume solid-phase support obtained from Glen Research. Standard synthesis cycles provided by Applied Biosystems were used for all normal bases using 2 min coupling times. The coupling time was increased to 10 min for the positions at which the caged deoxythymidine modified phosphoramidites were incorporated. The caged dumbbell triplex-forming oligonucleotides were synthesized using the 0.2 μM scale with 1000 Å solid phase supports obtained from Glen Research. Reagents for automated DNA synthesis were also obtained from Glen Research. The NPE-caged deoxycytidine phosphoramidite was resuspended in anhydrous acetonitrile to a concentration of 0.1 M. Standard synthesis cycles provided by Applied Biosystems with 25 s coupling times were used for all bases.

Gel Shift Assays. Gel shift assays were performed as previously described.[32] In short, cyclin D1 target sense strand was 5′ radiolabeled with ^{32}P-γ ATP (MP Biomedicals) and annealed to its complementary strand. A 5-fold excess of TFO (500 nM) was incubated with the radiolabeled duplex (100 nM) in TBM (89 mM Tris, 89 mM boric acid, 10 mM $MgCl_2$, pH 7.4) buffer at 37 °C for 4 h. Aliquots were kept in the dark or irradiated for 2 min (CHP-TFO-1) or 5 min (CBD-TFOs) using a transilluminator (365 nm, 25 W). After irradiation, the TFO/dsDNA target mixtures were incubated for 30 min at 30 °C and analyzed on a 16% TBM gel and imaged with a Typhoon FLA 7000.

TFO Inhibition of Gene Expression in Mammalian Cells. Human embryonic kidney (HEK) 293T cells were grown at 37 °C, 5% CO_2 in Dulbecco's modified Eagle's medium (Hyclone), supplemented with 10% fetal bovine serum (Hyclone) and 10% streptomycin/penicillin (MP Biomedicals). Cells were passaged into a 96-well plate (200 μL per well, ~1 × 10^4 cells per well) and grown to ~70% confluence within 24 h. The medium was changed to Optimem (Invitrogen), and the cells were co-transfected with pCyclin D1 Δ-944 (0.15 μg, gift from Dr. Linda Schuler, University of Wisconsin, Madison), pRL-TK (0.15 μg, Promega), and TFO DNA (0.5 μM) using X-tremeGene (3:2 reagent/DNA ratio, Roche). All transfections were performed in triplicate. Cells were incubated at 37 °C for 4 h, the transfection medium was removed and replaced with standard growth medium, and the cells were incubated for an additional 24 h. After the 24 h incubation, the medium was removed, and the cells were assayed with a Dual-Luciferase Reporter Assay system (Promega) using a Biotek Synergy 4 microplate reader. The firefly luciferase signal was normalized to the *Renilla* luciferase signal for each of the triplicates, the data were averaged, and standard deviations were calculated.

Light Regulation of TFOs. HEK 293T cells were passaged into a 96-well plate (200 μL per well, ~1 × 10^4 cells per well) and grown to ~70% confluence within 24 h. The medium was changed to Optimem, and the cells were co-transfected with pCyclin D1 Δ-944 (0.15 μg), pRL-TK (0.15 μg, Promega), and TFO DNA (0.5 μM) using X-tremeGene. All transfections were performed in triplicate. Cells were incubated at 37 °C for 4 h, and the transfection medium was removed. Selected wells were briefly irradiated with a transilluminator (365 nm, 25 W) for 2 min (CHP-TFO-1) or 5 min (CBD-TFOs). The medium was then replaced with standard growth medium, and the cells were incubated for an additional 24 h. After the 24 h incubation, the medium was removed, and the cells were assayed with a Dual-Luciferase Reporter Assay system using a Biotek Synergy 4 microplate reader. Firefly luciferase signal was normalized the *Renilla* luciferase signal for each of the triplicates, the data was averaged, and standard deviations were calculated.

Quantitative RT-PCR. MDA-MB-231 cells were passaged into 6-well plates (2 mL per well, ~ 2 × 10^5 cells per well) and grown to ~70% confluence within 24 h. The medium was changed to Optimem (Invitrogen), and the cells were transfected with 0.5 μM TFOs using X-tremeGENE transfection reagent (3:2 reagent/RNA ratio, Roche). Cells were incubated at 37 °C for 4 h, the transfection medium was removed, and 1 mL of PBS (pH 7.4) was added. The cells were irradiated for 5 min on a UV transilluminator (365 nm, 25W). DMEM media was added, the cells were incubated at 37 °C, 5% CO_2 for 48 h. RNA was isolated with TRIZOL reagent (Invitrogen). cDNAs were synthesized with Superscript Reverse Transcriptase II (Invitrogen), and quantitative RT PCRs were performed with cyclin D1 forward primer 5′ CCTGTCCTACTACCGCCTCA, cyclin D1 reverse primer 5′ CAGTCCGGGTCACACTTGA,[61] GAPDH forward primer 5′ TGCACCACCAACTGCTTAGC, and GAPDH reverse primer 5′ GGCATGGACTGTGGTCATGAG. The threshold cycles (Ct) of each sample were normalized to the GAPDH housekeeping gene and relative to untreated cells. For each of the triplicates, the data was averaged, and standard deviations were calculated.

2-(1-(6-Nitrobenzo[*d*][1,3]dioxol-5-yl)ethyl)isoindoline-1,3-dione (2). To a stirring solution of the alcohol **1** (2.0 g, 9.4 mmol) in THF (25 mL) at 0 °C under an argon atmosphere were added phthalimide (1.4 g, 9.4 mmol) and triphenylphosphine (2.9 g, 11.2 mmol). Diisopropyl azodicarboxylate (2.20 mL, 11.2 mmol) was slowly added into the reaction mixture at 0 °C and was stirred for another 4 h at RT. The solvent was removed under reduced pressure, and the residue was diluted with CH_2Cl_2 (20 mL). The organic layer was washed with a saturated aqueous solution of $NaHCO_3$ (2 × 20 mL) and brine (20 mL), dried over anhydrous Na_2SO_4, and evaporated under reduced pressure. The thus obtained residue was purified by column chromatography on silica gel using CH_2Cl_2/hexanes (1:4) to afford the dione **2** (2.4 g, 77% yield) as a white solid. ^{1}H NMR (400 MHz, $CDCl_3$): δ 7.79−7.76 (m, 2H), 7.69−7.66 (m, 2H), 7.34−7.31 (m, 2H), 6.08−6.04 (m,, 3H), 1.91 (d, J = 6.8 Hz, 3H). ^{13}C NMR (100 MHz, $CDCl_3$): δ 168.3, 151.8, 147.4, 143.1, 134.3, 132.5, 131.8, 123.5, 108.7, 105.4, 103.1, 46.4, 18.8. HRMS-ESI (m/z) [M + Na]$^+$ calcd for $C_{17}H_{12}N_2O_6$ 363.0588, found 363.0592.

1-(6-Nitrobenzo[*d*][1,3]dioxol-5-yl)ethanamine (3). To a stirring solution of the dione **2** (2.4 g, 7.0 mmol) in dry EtOH (30 mL) at RT under an argon atmosphere was slowly added NH_2NH_2 (0.55 mL, 17.6 mmol), and the mixture was refluxed for 1 h. The reaction mixture was then cooled to 0 °C for 15 min, and diethyl ether (200 mL) was added while stirring vigorously. The formed precipitate was filtered off and washed with diethyl ether (10 × 5 mL). The residue was purified by column chromatography on silica gel using CH_2Cl_2/MeOH (9:1) with 1% TEA to obtain the amine **3** (1.2 g, 81% yield) as a yellow solid. ^{1}H NMR (300 MHz, $CDCl_3$): δ 7.32 (s, 1H), 7.22 (s, 1H), 6.06 (dd, 2H), 4.63 (q, J = 6.6 Hz, 1H), 1.59 (s, 2H), 1.37 (d, J = 6.6 Hz, 3H). ^{13}C NMR (75 MHz, $CDCl_3$): δ 152.1, 146.5,

dx.doi.org/10.1021/cb300161r | ACS Chem. Biol. XXXX, XXX, XXX−XXX

139.8, 106.5, 105.1, 102.9, 46.2, 24.8. HRMS-ESI (m/z) $[M + H]^+$ calcd for $C_9H_{10}N_2O_4$ 211.0713, found 211.0717.

1-((2*R*,4*S*,5*R*)-4-((*tert*-Butyldimethylsilyl)oxy)-5-(((*tert* butyldimethylsilyl)oxy)methyl)tetrahydrofuran-2-yl)-4-((1-(6-nitrobenzo[*d*][1,3]dioxol-5-yl)ethyl)amino)pyrimidin-2(1*H*)-one (5). To a stirring solution of the sulfonate **4** (1.0 g, 1.3 mmol) in dry DMF (5 mL) at RT under an argon atmosphere was slowly added DIPEA (0.72 mL, 4.4 mmol) followed by the amine **3** (0.58 g, 2.7 mmol). The reaction mixture was then heated to 90 °C overnight. The reaction mixture was cooled to RT, poured into a saturated aqueous solution of $NaHCO_3$ (30 mL), and extracted using EtOAc (3 × 20 mL). The combined organic layer was washed with saturated aqueous solution of $NaHCO_3$ (3 × 10 mL) and brine (10 mL) and dried over anhydrous Na_2SO_4. The solvent was evaporated under reduced pressure, and the residue was purified by column chromatography on silica gel using EtOAc with 1% TEA to obtain compound **5** (0.80 g, 89% yield) as a pale yellow solid. ^{1}H NMR (400 MHz, CD_3COCD_3): δ 7.82 (dd, J = 24 Hz, 7.6 Hz, 1H), 7.58 (br, 1H), 7.43 (s, 1H), 7.14 (d, J = 12 Hz, 1H), 6.20−6.16 (m, overlap, 3H), 5.82 (dd, J = 24 Hz, 7.6 Hz, 1H), 5.73 (br, 1H), 4.47 (br, 1H), 3.90−3.83 (m, overlap, 3H), 2.31−1.99 (m, 2H), 1.53 (d, J = 6.8 Hz, 3H), 0.93−0.88 (m, 18 H), 0.12−0.08 (m, 12 H). ^{13}C NMR (100 MHz, CD_3COCD_3): δ 163.7, 155.7, 155.6, 153.2, 153.1, 141.0, 139.2, 139.0, 106.9, 106.7, 105.6, 105.5, 104.2, 94.9, 94.8, 88.1, 86.3, 72.5, 72.3, 63.4, 63.3, 47.2, 47.0, 42.3, 42.2, 26.3, 26.1, 22.3, 18.9, 18.5, −4.4, −4.6, −5.2, −5.3. HRMS-ESI (m/z) $[M + H]^+$ calcd for $C_{30}H_{48}N_4O_8Si_2$ 649.3083, found 649.3081.

1-((2*R*,4*S*,5*R*)-4-Hydroxy-5-(hydroxymethyl)tetrahydrofuran-2-yl)-4-((1-(6-nitrobenzo[*d*][1,3]dioxol-5-yl)ethyl)amino)-pyrimidin-2(1*H*)-one (6). To a stirring solution of compound **5** (0.80 g, 1.2 mmol) in dry THF (15 mL) at 0 °C was slowly added a 1.0 M solution of TBAF (3.6 mL, 3.6 mmol). After 30 min, the ice bath was removed, and the reaction mixture was stirred for another 3 h at RT. The solvent was removed under reduced pressure, and the residue was purified by column chromatography on silica gel using CH_2Cl_2/MeOH (9:1) with 1% TEA to yield compound **6** (0.48 g, 95% yield) as a white solid. ^{1}H NMR (300 MHz, DMSO-d_6): δ 8.26−8.24 (m, 1H), 7.77 (d, J = 7.2 Hz, 1H), 7.54 (s, 1H), 7.09 (d, J = 3, 1H), 6.19−6.17 (m, 2H), 6.09−6.03 (m, 1H), 5.79 (d, J = 7.5 Hz, 1H), 5.55−5.49 (m, 1H), 5.19 (t, J = 3.6 Hz, 1H), 4.93 (t, J = 5.4 Hz, 1H), 4.16 (br, 1H), 3.74 (br, 1H), 3.51 (br, 2H), 2.12−2.01 (m, 1H), 1.94−1.82 (m, 1H), 1.45 (d, J = 6.8 Hz, 3H). ^{13}C NMR (100 MHz, DMSO-d_6): δ 162.2, 154.6, 151.9, 146.4, 141.6, 140.5, 137.7, 105.7, 105.6, 104.6, 104.3, 94.3, 87.2, 84.9, 70.4, 70.3, 61.3, 45.3, 45.2, 21.9, 21.8. HRMS-ESI (m/z) $[M + H]^+$ calcd for $C_{18}H_{20}N_4O_8$ 421.1354, found 421.1358.

1-((2*R*,4*S*,5*R*)-5-((Bis(4-methoxyphenyl)(phenyl)methoxy)-methyl)-4-hydroxytetrahydrofuran-2-yl)-4-((1-(6-nitrobenzo-[*d*][1,3]dioxol-5-yl)ethyl)amino)pyrimidin-2(1*H*)-one (7). To a stirring solution of compound **6** (0.20 g, 0.47 mmol) in dry pyridine (1.0 mL) at RT was added DMTCl (0.19 g, 0.57 mmol). After 12 h, MeOH (0.2 mL) was added into the reaction mixture in order to quench unreacted DMTCl. The solvent was removed under reduced pressure, and the residue was dissolved in dichloromethane (15 mL). The organic layer was washed with 5% citric acid (2 × 5 mL), saturated aqueous solution of $NaHCO_3$ (5 mL), and brine (5 mL) and dried over anhydrous Na_2SO_4. The solvent was evaporated under reduced pressure, and the obtained residue was purified by column chromatography on silica gel using CH_2Cl_2/MeOH (20:1) with 1% TEA to give compound **7** (0.26 g, 72% yield) as a white solid. ^{1}H NMR (300 MHz, CD_3COCD_3): δ 8.02 (s, 1H), 7.81−7.76 (m, 1H), 7.52−7.43 (m, 3H), 7.34−28 (m, 6H), 7.24−7.11 (m, 2H), 6.89−6.86 (m, 4H), 6.24−6.15 (m, 3H), 5.74−5.65 (m, 2H), 4.50−4.47 (m, 2H), 4.01−3.99 (m, 1H), 3.78 (s, 6H), 3.35 (d, J = 2.7 Hz, 2H), 2.34−2.28 (m, 1H), 2.15−2.09 (m, 1H), 1.52 (d, J = 6.8 Hz, 3H). ^{13}C NMR (100 MHz, CD_3COCD_3): δ 163.8, 159.6, 155.7, 153.2, 153.1, 147.6, 146.0, 143.2, 141.1, 139.1, 139.0, 136.7, 136.5, 131.0, 129.0, 128.6, 127.6, 113.9, 106.8, 106.7, 105.6, 104.2, 94.8, 87.2, 86.8, 86.4, 86.3, 79.2, 71.6, 71.5, 64.2, 55.5, 47.2, 47.0, 42.1, 42.0, 22.3. HRMS-ESI (m/z) $[M + H]^+$ calcd for $C_{39}H_{38}N_4O_{10}$ 723.2661, found 723.2658.

(2*R*,3*S*,5*R*)-2-((Bis(4-methoxyphenyl)(phenyl)methoxy)-methyl)-5-(4-((1-(6-nitrobenzo[*d*][1,3]dioxol-5-yl)ethyl)amino)-2-oxopyrimidin-1(2*H*)-yl)tetrahydrofuran-3-yl (2-cyanoethyl) diisopropylphosphoramidite (8). To a stirring solution of compound **7** (0.20 g, 0.27 mmol) in dry dichloromethane (2 mL) at 0 °C under an argon atmosphere were added DIPEA (0.24 mL, 1.38 mmol) and 2-cyanoethyl-*N*,*N*-diisopropylchlorophosphoramidite (0.12 mL, 0.55 mmol). After 20 min, the ice bath was removed, and the reaction mixture was stirred for another 2 h at RT. The solvent was removed under reduced pressure, and the residue was purified by column chromatography on silica gel using $CHCl_3$/CH_3COCH_3 (20:1) with 1% TEA to afford a white solid. The white solid was dissolved in dichloromethane (0.5 mL) and precipitated in diethyl ether (20 mL) in order to remove the excess of chlorophosphoramidite reagent that was coeluted with the desired product. The precipitate was filtered to obtain the phosphoramidite **8** (0.11 g, 45% yield) as an off white solid. ^{1}H NMR (400 MHz, CD_3COCD_3): δ 7.84−7.78 (m, 1H), 7.48−7.44 (m, 4H), 7.36−7.32 (m, 6H), 7.24−7.22 (m, 1H), 7.12 (d, J = 12 Hz, 1H), 6.90−6.87 (m, 4H), 6.27−6.16 (m, 3H), 5.74−5.71 (m, 1H), 5. 68−5.66 (m, 1H), 4.65 (br, 1H), 4.14−4.09 (m, 1H), 3.70 (br, 6H), 3.72−3.54 (m, 2H), 3.42−3.35 (m, 2H), 2.76−272 (m, 1H), 2.63−2.60 (m, 1H), 2.52−2.39 (m, 1H), 2.28−2.16 (m, 1H), 1.53 (d, J = 6.8 Hz, 3H), 1.27−0.83 (m, 12 H). ^{13}C NMR (100 MHz, CD_3COCD_3): δ 163.7, 159.7, 155.4, 151.7, 145.9, 141.1, 136.5, 131.0, 129.0, 128.7, 127.7, 114.0, 106.8, 106.7, 105.6, 104.3, 94.9, 87.3, 86.4, 63.9, 59.6, 59.4, 55.5, 47.0, 46.9, 43.9, 43.8, 41.0, 24.9, 24.8, 22.2, 20.7. ^{13}P NMR (121 MHz, CD_3COCD_3, reference H_3PO_4 = 0.00 ppm): δ 146.55, 146.50 146.39, 146.34.

■ ASSOCIATED CONTENT

Ⓢ Supporting Information

Optimization of transfection conditions, luciferase assay conditions, and UV irradiation; NMR spectra of synthesized compounds. This material is available free of charge via the Internet at http://pubs.acs.org.

■ AUTHOR INFORMATION

Corresponding Author

*E-mail: alex_deiters@ncsu.edu.

Notes

The authors declare no competing financial interest.

■ ACKNOWLEDGMENTS

This research was supported in part by the National Institutes of Health (R01GM079114). We would like to thank L. Schuler (University of Wisconsin, Madison) for the pCyclin D1 Δ-944 plasmid.

■ REFERENCES

(1) Jain, A., Magistri, M., Napoli, S., Cabone, G. M., and Catapano, C. V. (2010) Mechanisms of triplex DNA-mediated inhibition of transcription initiation in cells. *Biochimie 92*, 317−320.

(2) Guntaka, R. V., Varma, B. R., and Weber, K. T. (2003) Triplex-forming oligonucleotides as modulators of gene expression. *Int. J. Biochem. Cell Biol. 35*, 22−31.

(3) Diviacco, S., Rapozzi, V., Xodo, L., Helene, C., Quadrifoglio, F., and Giovannangeli, C. (2001) Site-directed inhibition of DNA replication by triple helix formation. *FASEB J. 15*, 2660−2668.

(4) Oussedik, K., François, J. C., Halby, L., Senamaud-Beaufort, C., Toutirais, G., Dallavalle, S., Pommier, Y., Pisano, C., and Arimondo, P. B. (2010) Sequence-specific targeting of IGF-I and IGF-IR genes by camptothecins. *FASEB J. 24*, 2235−2244.

(5) Liu, Y., Nairn, R. S., and Vasquez, K. M. (2008) Processing of triplex-directed psoralen DNA interstrand crosslinks by recombination mechanisms. *Nucleic Acids Res. 36*, 4680−4688.

(6) Simon, P., Cannata, F., Concordet, J. P., and Giovannangeli, C. (2008) Targeting DNA with triplex-forming oligonucleotides to modify gene sequence. *Biochimie 90*, 1109−1116.
(7) Vasquez, K. M., and Glazer, P. M. (2002) Triplex-forming oligonucleotides: principles and applications. *Q. Rev. Biophys. 35*, 89−107.
(8) Patterson, A., Caprio, F., Vallée-Bélisle, A., Moscone, D., Plaxco, K. W., Palleschi, G., and Ricci, F. (2010) Using triplex-forming oligonucleotide probes for the reagentless, electrochemical detection of double-stranded DNA. *Anal. Chem. 82*, 9109−9115.
(9) Seidman, M., and Glazer, P. (2003) The potential for gene repair via triple helix formation. *J. Clin. Invest. 112*, 487−494.
(10) Tomita, N., Tomita, T., Yuyama, K., Tougan, T., Tajima, T., Ogihara, T., and Morishita, R. (2003) Development of novel decoy oligonucleotides: advantages of circular dumb-bell decoy. *Curr. Opin. Mol. Ther. 5*, 107−112.
(11) Schleifman, E., Chin, J., and Glazer, P. (2008) Triplex-mediated gene modification. *Methods Mol. Biol. 435*, 175−190.
(12) Jain, A., Wang, G., and Vasquez, K. M. (2008) DNA triple helices: biological consequences and therapeutic potential. *Biochimie 90*, 1117−1130.
(13) Riggsbee, C. W., and Deiters, A. (2010) Recent advances in the photochemical control of protein function. *Trends Biotechnol 28*, 468−475.
(14) Deiters, A. (2010) Principles and Applications of the Photochemical Control of Cellular Processes. *ChemBioChem 11*, 47−53.
(15) Deiters, A. (2009) Light activation as a method of regulating and studying gene expression. *Curr. Opin. Chem. Biol. 13*, 678−686.
(16) Lee, H. M., Larson, D. R., and Lawrence, D. S. (2009) Illuminating the chemistry of life: design, synthesis, and applications of "caged" and related photoresponsive compounds. *ACS Chem. Biol. 4*, 409−427.
(17) Meng, X. M., Chen, X. Y., Fu, Y., and Guo, Q. X. (2008) Photolysis of caged compounds and its applications to chemical biology. *Prog. Chem. 20*, 2034−2044.
(18) Dmochowski, I. J., and Tang, X. J. (2007) Taking control of gene expression with light-activated oligonucleotides. *Biotechniques 43*, 161−163.
(19) Mayer, G., and Heckel, A. (2006) Biologically active molecules with a "light switch". *Angew. Chem., Int. Ed. 45*, 4900−4921.
(20) Young, D. D., and Deiters, A. (2007) Photochemical control of biological processes. *Org. Biomol. Chem. 5*, 999−1005.
(21) Deiters, A., Garner, R. A., Lusic, H., Govan, J. M., Dush, M., Nascone-Yoder, N. M., and Yoder, J. A. (2010) Photocaged morpholino oligomers for the light-regulation of gene function in zebrafish and Xenopus embryos. *J. Am. Chem. Soc. 132*, 15644−15650.
(22) Richards, J. L., Seward, G. K., Wang, Y. H., and Dmochowski, I. J. (2010) Turning the 10−23 DNAzyme on and off with light. *ChemBioChem 11*, 320−324.
(23) Casey, J. P., Blidner, R. A., and Monroe, W. T. (2009) Caged siRNAs for spatiotemporal control of gene silencing. *Mol. Pharmaceutics 6*, 669−685.
(24) Young, D. D., Lusic, H., Lively, M. O., Yoder, J. A., and Deiters, A. (2008) Gene silencing in mammalian cells with light-activated antisense agents. *ChemBioChem 9*, 2937−2940.
(25) Young, D. D., Edwards, W. F., Lusic, H., Lively, M. O., and Deiters, A. (2008) Light-triggered polymerase chain reaction. *Chem. Commun.*, 462−464.
(26) Buchakjian, M. R., and Kornbluth, S. (2010) The engine driving the ship: metabolic steering of cell proliferation and death. *Nat. Rev. Mol. Cell Biol. 11*, 715−727.
(27) Caldon, C. E., Sutherland, R. L., and Musgrove, E. (2010) Cell cycle proteins in epithelial cell differentiation: implications for breast cancer. *Cell Cycle 9*, 1918−1928.
(28) Diehl, J. A. (2002) Cycling to cancer with cyclin D1. *Cancer Biol. Ther. 1*, 226−231.
(29) Kim, J. K., and Diehl, J. A. (2009) Nuclear cyclin D1: an oncogenic driver in human cancer. *J. Cell Physiol. 220*, 292−296.
(30) Tashiro, E., Tsuchiya, A., and Imoto, M. (2007) Functions of cyclin D1 as an oncogene and regulation of cyclin D1 expression. *Cancer Sci. 98*, 629−635.
(31) Shuai, X., Han, G., and Wang, G. (2003) Effects of cyclin D1 antisense oligodeoxyneucleotides on the growth and expression of G1 phase regulators in gastric carcinoma cells. *J. Huazhong Univ. Sci. Technol., Med. Sci. 23* (396−398), 406.
(32) Kim, H. G., and Miller, D. M. (1998) A novel triplex-forming oligonucleotide targeted to human cyclin D1 (bcl-1, proto-oncogene) promoter inhibits transcription in HeLa cells. *Biochemistry 37*, 2666−2672.
(33) Shuai, X. M., Han, G. X., Wang, G. B., and Chen, J. H. (2006) Cyclin D1 antisense oligodexoyneucleotides inhibits growth and enhances chemosensitivity in gastric carcinoma cells. *World J. Gastroenterol. 12*, 1766−1769.
(34) Young, D., Lively, M., and Deiters, A. (2010) Activation and deactivation of DNAzyme and antisense function with light for the photochemical regulation of gene expression in mammalian cells. *J. Am. Chem. Soc. 132*, 6183−6193.
(35) Young, D. D., Govan, J. M., Lively, M. O., and Deiters, A. (2009) Photochemical regulation of restriction endonuclease activity. *ChemBioChem 10*, 1612−1616.
(36) Lusic, H., Young, D. D., Lively, M. O., and Deiters, A. (2007) Photochemical DNA activation. *Org. Lett. 9*, 1903−1906.
(37) Cooney, M., Czernuszewicz, G., Postel, E. H., Flint, S. J., and Hogan, M. E. (1988) Site-specific oligonucleotide binding represses transcription of the human c-myc gene in vitro. *Science 241*, 456−459.
(38) Ye, Z., Guntaka, R. V., and Mahato, R. I. (2007) Sequence-specific triple helix formation with genomic DNA. *Biochemistry 46*, 11240−11252.
(39) Carbone, G. M., McGuffie, E. M., Collier, A., and Catapano, C. V. (2003) Selective inhibition of transcription of the Ets2 gene in prostate cancer cells by a triplex-forming oligonucleotide. *Nucleic Acids Res. 31*, 833−843.
(40) Besch, R., Giovannangeli, C., Kammerbauer, C., and Degitz, K. (2002) Specific inhibition of ICAM-1 expression mediated by gene targeting with Triplex-forming oligonucleotides. *J. Biol. Chem. 277*, 32473−32479.
(41) Eckstein, F. (2000) Phosphorothioate oligodeoxynucleotides: what is their origin and what is unique about them? *Antisense Nucleic Acid Drug Dev. 10*, 117−121.
(42) Eckstein, F., and Gish, G. (1989) Phosphorothioates in molecular biology. *Trends Biochem. Sci. 14*, 97−100.
(43) Abdelgany, A., Wood, M., and Beeson, D. (2007) Hairpin DNAzymes: a new tool for efficient cellular gene silencing. *J. Gene Med. 9*, 727−738.
(44) Herber, B., Truss, M., Beato, M., and Muller, R. (1994) Inducible regulatory elements in the human cyclin-D1 promoter. *Oncogene 9*, 1295−1304.
(45) Eder, P. S., DeVine, R. J., Dagle, J. M., and Walder, J. A. (1991) Substrate specificity and kinetics of degradation of antisense oligonucleotides by a 3′ exonuclease in plasma. *Antisense Res. Dev. 1*, 141−151.
(46) Cogoi, S., Rapozzi, V., Quadrifoglio, F., and Xodo, L. (2001) Anti-gene effect in live cells of AG motif triplex-forming oligonucleotides containing an increasing number of phosphorothioate linkages. *Biochemistry 40*, 1135−1143.
(47) Heckel, A., Buff, M. C., Raddatz, M. S., Müller, J., Pötzsch, B., and Mayer, G. (2006) An anticoagulant with light-triggered antidote activity. *Angew. Chem., Int. Ed. 45*, 6748−6750.
(48) Bochet, C. (2000) Wavelength-selective cleavage of photolabile protecting groups. *Tetrahedron Lett. 41*, 6341−6346.
(49) Holmes, C. P. (1997) Model studies for new o-nitrobenzyl photolabile linkers: Substituent effects on the rates of photochemical cleavage. *J. Org. Chem. 62*, 2370−2380.
(50) Park, S., Bando, T., Shinohara, K., Nishijima, S., and Sugiyama, H. (2011) Photocontrollable sequence-specific DNA alkylation by a pyrrole-imidazole polyamide seco-CBI conjugate. *Bioconjugate Chem. 22*, 120−124.

(51) Anderson, E., Brown, T., and Picken, D. (2003) Novel photocleavable universal support for oligonucleotide synthesis. *Nucleosides Nucleotides Nucleic Acids 22*, 1403−1406.
(52) Höbartner, C., and Silverman, S. K. (2005) Modulation of RNA tertiary folding by incorporation of caged nucleotides. *Angew. Chem., Int. Ed. 44*, 7305−7309.
(53) Schäfer, F., Joshi, K. B., Fichte, M. A., Mack, T., Wachtveitl, J., and Heckel, A. (2011) Wavelength-selective uncaging of dA and dC residues. *Org. Lett. 13*, 1450−1453.
(54) Lusic, H., Lively, M. O., and Deiters, A. (2008) Light-activated deoxyguanosine: photochemical regulation of peroxidase activity. *Mol. Biosyst. 4*, 508−511.
(55) Mojzísek, M. (2004) Triplex forming oligonucleotides--tool for gene targeting. *Acta Med. (Hradec Kralove, Czech Repub.) 47*, 151−156.
(56) Duca, M., Vekhoff, P., Oussedik, K., Halby, L., and Arimondo, P. B. (2008) The triple helix: 50 years later, the outcome. *Nucleic Acids Res. 36*, 5123−5138.
(57) Arya, D. P. (2011) New approaches toward recognition of nucleic acid triple helices. *Acc. Chem. Res. 44*, 134−146.
(58) Semenyuk, A., Darian, E., Liu, J., Majumdar, A., Cuenoud, B., Miller, P. S., Mackerell, A. D., and Seidman, M. M. (2010) Targeting of an interrupted polypurine:polypyrimidine sequence in mammalian cells by a triplex-forming oligonucleotide containing a novel base analogue. *Biochemistry 49*, 7867−7878.
(59) Kuan, J. Y., and Glazer, P. M. (2004) Targeted gene modification using triplex-forming oligonucleotides. *Methods Mol. Biol. 262*, 173−194.
(60) Vasquez, K. M., Narayanan, L., and Glazer, P. M. (2000) Specific mutations induced by triplex-forming oligonucleotides in mice. *Science 290*, 530−533.
(61) Tobin, N. P., Sims, A. H., Lundgren, K. L., Lehn, S., and Landberg, G. (2011) Cyclin D1, Id1 and EMT in breast cancer. *BMC Cancer 11*, 417.